Leaf nitrogen determination of corn plant using aerial images and artificial neural networks*

R.K. Gautam and S. Panigrahi**

Agricultural and Biosystems Engineering Department, North Dakota State University, Fargo, North Dakota 58105-5626, USA.
***Email: s.panigrahi@ndsu.edu*

Gautam, R.K. and Panigrahi, S. 2007. **Leaf nitrogen determination of corn plant using aerial images and artificial neural networks**. Canadian Biosystems Engineering/Le génie des biosystèmes au Canada **49**: 7.1 - 7.9. Image processing techniques were developed to extract statistical and textural features from multi-spectral bands of aerial images. Along with the conventional image bands of red, green, and near-infrared, two additional image bands, normalized difference vegetation index (NDVI) and green vegetation index (GVI) were derived. Two neural network architectures, multilayer perceptron and radial basis function were applied to develop twenty neural network (NN) models for predicting leaf nitrogen content of corn plants in field conditions. The extracted image features were used as input to the neural network models. Performance of the neural network models were evaluated based on simultaneous comparison of root mean square error of prediction (RMSEP), minimum prediction accuracy (MPA), and correlation coefficient. The optimum NN model was based on the radial basis function architecture and used textural image features as its inputs. The radial basis function based on green vegetation index texture (RBGvT) provided an RMSEP of 6.6%, MPA of 88.8%, and correlation coefficient of 78% for predicting leaf nitrogen content in field conditions. **Keywords:** leaf nitrogen, image processing, neural network, precision farming, corn.

Des techniques de traitement d'images ont été développées pour extraire des caractéristiques statistiques et texturales à partir de bandes multispectrales d'images aériennes. En plus des bandes conventionnelles d'images dans le rouge, le vert et l'infrarouge rapproché, deux bandes visuelles ont été dérivées soit l'indice de végétation à différence normalisée, 'NDVI', et les indices globaux de végétations ('GVI'). Deux architectures de réseaux neuronaux soit, le perceptron multicouches et la fonction à base radiale, ont été utilisées pour développer vingt modèles de réseaux neuronaux pour la prédiction du contenu en azote foliaire des plants de maïs au champ. Les caractéristiques extraites des images ont été utilisées comme intrants pour les modèles de réseaux neuronaux. La performance des modèles de réseaux neuronaux a été évaluée en réalisant des comparaisons simultanées de l'erreur brute ('RMSEP'), la précision de prédiction minimale ('MPA') et le coefficient de corrélation. Le modèle optimum NN était basé sur une architecture de fonction de base radiale et des caractéristiques de texture d'image utilisées comme intrants au modèle. La fonction de base radiale basée sur la texture de l'index de végétation ('RBGvT') a permis d'obtenir un RMSEP de 6,6%, un MPA de 88,8% et un coefficient de corrélation de 78% pour la prédiction du contenu en azote foliaire. **Mots clés**: azote foliaire, analyse d'image, réseau neuronal, agriculture de précision, maïs.

*Based on "Image processing techniques and neural network models for predicting plant nitrate using aerial images," by Ramesh Kumar Gautam and Suranjan Panigrahi. Proceedings of International Joint Conference on Neural Network (IJCNN-IEEE), held in Portland, Oregon, USA, July 20-24, 2003.

INTRODUCTION

Nitrogen is a critical nutrient for the growth of healthy vegetation. Proper management of nitrogen application helps to optimize crop uptake and reduces nitrogen losses to the wider environment. The nitrogen utilized by crops depends largely on the availability of the inorganic form of nitrogen, which may constitute approximately 0.1% of total nitrogen in the soil (Sauchelli 1964). Part of the absorbed nitrogen is stored in plant leaves in the form of vegetation vigor. Hence, determination of plant nitrogen is crucial to optimize crop yield, while at the same time minimizing negative environmental impacts.

Various techniques have been used to quantify leaf nitrogen content under laboratory as well as field conditions. For example, leaf nitrogen can be determined by measuring nitrate concentration in the laboratory (Filella et al. 1994; Greenwood et al. 1991). Studies were also performed to assess the relationship between chlorophyll and leaf nitrogen content (Hong et al. 1997; Flowers et al. 2000). The correlation between chlorophyll and nitrogen of paddy leaves ranged between 0.90 and 0.94 (Hong et al. 1997). Leaf nitrogen was also determined using leaf canopy reflectance (Flowers et al. 2000; Reeves et al. 1993; Scharf and Lory 2000; Viets and Hageman 1971). The coefficient of determination between plant nitrogen spectral index (PNSI) and nitrogen uptake at different spectral bands (red at 761 nm and near infrared at 780 nm) was found to be 0.67 (Stone et al. 1996). Leaf nitrogen content changes with crop growing stage (Huggins and Pan 1993; Zhuang and Bemard 1990) and also varies with ambient air temperature (Cihacek and Kerby 1991; Sauchelli 1964).

Leaf chlorophyll and nitrogen of corn was determined using airborne hyper-spectral and infrared remote sensing technique in field conditions (Beatty et al. 2000). They found more prominent variation of spectral response in green and near infrared (NIR) bands. Aerial photograph and spectral radiometer were used to calibrate leaf nitrogen status of a corn crop (Scharf and Lory 2000). Green band was found to be the potential predictor of side-dress nitrogen with a coefficient of determination of 0.51. Growing four popular corn hybrids with

varying rates of nitrogen fertilizer, Blackmer and White (1998) found that spectral reflectance (green at 550 nm and red at 710 nm) was related to leaf nitrogen with a correlation coefficient of 0.74. In a similar study, aerial images were used to compare the variability of leaf nitrogen deficiencies (Blackmer et al. 1996). Red band image was reported (Blackmer and White 1998; Scharf and Lory 2000) to provide higher correlation with nitrogen deficiencies. Variation of reflectance, transmittance, and absorption spectra of normal and nitrogen deficient corn leaves was separated by Al-Abbas et al. (1974). They found a correlation coefficient of 0.70 between plant moisture and percent absorbance.

The potentials of determining leaf nitrogen from the spectral characteristics at different spectral bands of visible and NIR spectrum were reported with a strong relationship between plant chlorophyll and leaf nitrogen (Huggins and Pan 1993; Stone et al. 1996). Nitrogen, when consumed by plants in the form of nitrate, changes to ammonia and subsequently to glutamine (Black 1999). The glutamine is a key enzyme for the development of protein in the leaves, thus, for the quantification of chlorophyll in plants (Black 1999). Previous studies have documented that chlorophyll affects spectral properties of light (Beatty et al. 2000; Flowers et al. 2000; Stone et al. 1996; Blackmer and White 1998; Blackmer et al. 1996; Scharf and Lory 2000). Therefore, spectral properties of plants, in the form of images, could contain features that might contain information about leaf nitrogen. Hence, we postulate that the spectral properties of plants in the form of statistical and textural image features could be helpful to predict leaf nitrogen under field conditions.

Selection of an appropriate technique is critical in obtaining a robust prediction model to be used in field conditions. Prior literature reveals the application of statistical techniques to develop prediction models (Al Aabbas et al. 1974; Blackmer and White 1998; Stone et al. 1996). Neural network, 'a form of artificial intelligence technique', has been used for several applications, including development of prediction models (Sérélé et al. 2000; O'Neal et al. 2002; Tumbo et al. 2002; Yang et al. 1996; Pachepsky et al. 1996; Drummond et al. 2002). Neural network has a greater ability to analyze rather complex data than others, e.g., statistical technique, particularly when the feature is complex and all data do not follow the similar distribution pattern (Benediktsson et al. 1990; Schalkoff 1992; Atkinson and Tatnall 1997). Moreover, the neural network technique incorporates a priori knowledge and realistic physical constraints into the analysis (Brown and Harris 1994; Foody 1995a, 1995b). Prior literature describes the use of various neural network architectures like multilayer perceptron (Thai and Shewfelt 1991; Foody 1995a; Tumbo et al. 2002; Pachepsky et al. 1996) and radial basis function (Huang 1999; Chen et al. 1991; Behloul et al. 2002). The selection of specific neural network architecture depends on the nature of the problem and data type.

The primary objective of this study was to develop neural network based models for predicting leaf nitrogen content of corn plant under field conditions using two neural network architectures (back propagation and radial basis function) and compare the performance of the models. The choice of the neural network architectures has been made based on their strength for prediction model buildings in real world conditions.

MATERIALS and METHODS

Image acquisition

We selected a portion of the best management practice (BMP) research site at Oakes (46° 3' 7.11" N, 98° 6' 42.76" W and 46° 2' 45.03" N, 98° 6' 6.68" W), North Dakota, as the field of our investigation. There were 68 plots, each measuring 171.13 m^2. Corn was planted in the summer of 2001 (June 10, 2001).

An aerial image of corn was acquired during the third week of July 2001 (July 22, 2001) using a Cessna aircraft flying at an approximate height of 1000 m at approximately 12:00 PM central standard time (CST) on a cloud-free sunny day. The images were acquired in both visible (400-700 nm) and NIR (700-900 nm) bands of the electromagnetic spectrum using a SLM 35-mm camera loaded with 100 ASA Ektachrome slide film. The spatial resolutions of the acquired images were 1 m in visible as well as *NIR* bands. The slides were scanned with a Nikon Scanner at 2800 dot per inch resolution and the digital images were saved in 'tiff' format.

Thirty corn leaves were collected from 10 plants at each plot in order to assess the leaf nitrogen content under field conditions. The corn leaves were collected at the same time (July 22, 2001, 12:00 PM CST) as image acquisition. The nitrogen content of the leaves was determined using the Kjeldahl nitrogen extraction procedure (Black 1999) at North Dakota State University. The nitrogen content was expressed as a percentage of total leaves weight.

Image processing

The aerial image was imported into a PC window platform and processed using Idrisi image processing software (Idrisi 32.11 2000, Worcester, MA). The visible and *NIR* band images were geo-referenced in WGS 84 reference coordinate system. The visible band image was split into red (R), green (G), and blue (B) bands. Only red and green band images from visible band and *NIR* band image from *NIR* band were used for further image processing and feature extraction. In addition, two additional images were derived using red, green, as well as *NIR* images and suitable band transformations. Two transformed images were (i) normalized difference vegetation index (*NDVI*) and (ii) green vegetation index (*GVI*). The *NDVI* image was computed using Eq. 1 (Goodin and Henebry 1997; Huemmrich and Goward 1997; Fernandez et al. 1997).

$$NDVI = \frac{NIR - R}{NIR + R} \tag{1}$$

where:

NDVI = normalized difference vegetation index and
NIR, R = near infrared and red band images, respectively.

Similarly, we computed the green vegetation index (*GVI*) band image using Eq. 2 (Gaston et al. 1997; Lecain et al. 2002).

$$GVI = \frac{NIR - G}{NIR + G} \tag{2}$$

where: G = green band images.

Statistical and textural feature extraction

Initially, green, red, *NIR*, *NDVI*, and *GVI* images were divided into 68 grid images as per end coordinates of each plot in the

research site. Global statistical image features i.e., mean (μ) and standard deviation (σ) were derived from each grid image. Textural indices are the image properties based on textural features or characteristics of the image (Haralick et al. 1973; Majumdar and Jayas 1999; Bogdanov et al. 2005), which show the variation of plant vegetation vigor (Sérélé et al. 2000). Different textural indices, such as homogeneity, contrast, and angular second moment (ASM), were used to predict corn yield (Sérélé et al. 2000). Therefore, textural indices from aerial images could predict leaf nitrogen. Thus, textural features were further extracted from each grid image corresponding to green, red, *NIR*, *GVI*, and *NDVI* bands. These extracted textural features were (i) diversity index (*H*), (ii) dominance index (*D*), (iii) fragmentation index (*F*), (iv) fractal dimension (*FD*), and (v) relative richness (*R*). Calculation of each textural index was made using a user defined window (of size 3x3) in each grid image.

Diversity Index (*H*) The Diversity Index shows how a specific gray-level value is distributed over the image. Variation of the nitrogen could cause different spatial patterns, which may be reflected in quantitative measure of diversity index (Monmonier 1974; Baldwin et al. 1996; Diker et al. 2004). Diversity index (H) of each grid image was computed as follows. Initially, the diversity index (H) value was computed as (Monmonier 1974; Idrisi 32.11 2000; Shackleton 2002):

$$H_w = -\sum_{x=1}^{k} P_x \log P_x \tag{3}$$

$$H = \sum_{w \in R} \frac{H_w}{N} \tag{4}$$

where:

H_w = diversity index of a window defined by the user (3x3), i.e., 9 pixels,
w = integer which represents the number of windows,
H = diversity index of the grid image,
N = total number of windows of the sub-image,
P_x = (number of pixels with gray levels, x)/(total number of pixels), and
k = 1.....256 (representing 256 gray levels).

Dominance Index (*D*) The Dominance Index shows the dominant pattern of the diversity index. Thus, for a window of size 3x3, the dominance index was calculated as the difference between maximum diversity of a specific window (among all windows within the grid image) and the diversity of the window under consideration. More specifically, it can be written as (Turner 1989; Idrisi 32.11 2000):

$$D_w = H_{w(\max)} - H_w \tag{5}$$

where: D_w = dominance index of a specific window.

Subsequently, the dominance index of the sub-image (*D*) was calculated using Eq. 6 (Turner 1989; Idrisi 32.11 2000).

$$D = \sum_{w \in R} \frac{D_w}{N} \tag{6}$$

The dominance index shows the relative variation of homogeneity over the region.

Fragmentation Index (*F*) The Fragmentation Index represents the relative variation of the gray level values over the total number of pixels in a window of a given size. More specifically, this index can be written as (Monmonier 1974; Idrisi 32.11 2000):

$$F_w = \frac{n-1}{c-1} \tag{7}$$

where:

F_w = fragmentation index for a window,
n = number of classes present in a window, and
c = total number of pixels in the window (Monmonier 1974).

The fragmentation index of a grid image was calculated as (Monmonier 1974; Idrisi 32.11 2000):

$$F = \sum_{w \in R} \frac{F_w}{N} \tag{8}$$

The fragmentation index shows how the homogeneity is distributed over a region of given grid image. Maximum value shows the extreme heterogeneity over the region. The more homogeneous the region is, the smaller the value of fragmentation index (Monmonier 1974).

Fractal Dimension (*FD*) The Fractal Dimension can serve as a useful measure of texture. It exhibits the property of statistical self-similarity. The fractal dimension of a window is described as (Critten 1997; Bettinger et al. 1996; Monmonier 1974; Idrisi 32.11 2000):

$$FD_w = \sum_{x=1}^{k} \log A_x \tag{9}$$

where:

FD_w = fractal dimension for a window and
A_x = area of a region with the same gray level values within a given window.

The Fractal Dimension of a grid image was determined using:

$$FD = \sum_{w \in R} \frac{FD_w}{N} \tag{10}$$

Relative Richness (*R*) The Relative Richness shows relative density of a specific gray level in a window over the maximum number of gray-level classes in a given grid image. Relative richness for a window of a given size is, therefore, defined as (Sheftel and Hanski 2002; Monmonier 1974; Idrisi 32.11 2000):

$$R_w = \frac{n_x}{n_{\max}} \times 100 \tag{11}$$

where:

R_w = relative richness for a window,
n_x = specific number of gray level class present in a 3x3 window, and
n_{max} = maximum possible number of gray level values in a given grid image.

The relative richness of the grid image was calculated as:

$$R = \sum_{w \in R} \frac{R_w}{N} \tag{12}$$

DEVELOPMENT OF NEURAL NETWORK MODELS

Multilayer perceptron and radial basis function neural network models

A multilayer perceptron with back propagation learning and a radial basis function neural network architecture were selected to develop models for predicting leaf nitrogen content of corn under field conditions. The multilayer perceptron with back propagation learning is a popular neural network architecture (Foody 1995a; Tumbo et al. 2002; Pachepsky et al. 1996; Plate et al. 2000; Pal et al. 2003; Bishop 1995; Cichocki and Unbehauen 1993). It has been used for a variety of applications including prediction, classification, system modeling, signal processing, noise filtering, etc. (Foody 1995a; Tumbo et al. 2002; Pachepsky et al. 1996; Plate et al. 2000; Pal et al. 2003; Bishop 1995; Cichocki and Unbehauen 1993). Compact representation is one of its advantages (Tumbo et al. 2002; Pachepsky et al. 1996; Plate et al. 2000; Pal et al. 2003; Bishop 1995; Cichocki and Unbehauen 1993; Honavar and Uhr 1994). In this paper, multilayer perceptron with back propagation learning is represented as a back propagation neural network (BPNN) model.

A typical multilayer perceptron neural network architecture has an input layer, one or more hidden layer(s), and an output layer. When the nodes of an input layer receive information from an external source, they become activated and emit signals to the next layer such that each node of the input layer has an exclusive correspondence to every node in the next layer (Cichocki and Unbehauen 1993; Honavar and Uhr 1994). These signals, in turn, pass to the output layer. Each connection between two nodes in adjacent layers is associated with weight coefficients, which adjust the signal strength based on the characteristic of input information (Cichocki and Unbehauen 1993). Depending on the strength, the signals reaching at each node can excite or inhibit the node (Cichocki and Unbehauen 1993; Honavar and Uhr 1994). During back propagation training, an error is determined by comparing the calculated output with the desired output and the error is propagated back to the hidden and input layers in subsequent trainings (Bishop 1995; Cichocki and Unbehauen 1993; Honavar and Uhr 1994). The training of the model is completed in a successive number of iterations when the change in error is sufficiently small (or less than the user defined limit). Additional information about the theory and development of back propagation neural networks (BPNN) can be found in (Tumbo et al. 2002; Pachepsky et al. 1996; Plate et al. 2000; Pal et al. 2003; Bishop 1995; Cichocki and Unbehauen 1993; Honavar and Uhr 1994).

A radial basis function neural network (RBFNN), on the other hand, is another popular architecture where fast training is one of its advantages. A typical RBFNN model consists of three successive layers fully connected by feed forward networks. A prototype layer, also called a hidden layer, is made up of higher dimensions to provide nonlinear transformation from the input layer. In general, RBFN implements Cover's theorem: "a complex pattern projected in high dimensional space non-linearly has higher likelihood to be linearly separable than in low dimensional space" (Hassoun 1995). Similar to the multilayer perceptron, each variable in its input layer has exclusive correspondence with every node in the prototype layer (Haykin 1994). There are no intermediate connections among the nodes in the prototype layer (Hanovar and Uhr 1994; Haykin 1994). During subsequent trainings, competition among the signals from the input layer form their own clusters based on a similarity criteria of the attributes (Bishop 1995; Cichocki and Unbehauen 1993; Honavar and Uhr 1994). These clusters represent the dominant information which passes to the output layer (Hassoun 1995). Moreover, there exists a linear transfer function between the prototype and output layer (Bishop 1995; Cichocki and Unbehauen 1993).

The output of the radial basis function neural network can be described as (Bishop 1995; Haykin 1994):

$$y_i(x) = \sum_{i=1}^{N} w_i f\left(\|x - c\|\right) \tag{13}$$

where:

$\{f(||x - c||)\ \ i = 1, 2, ..\ N\}$ = a set of N arbitrary functions and

w_i = randomized weight vector.

$\|x-c\|$ represents the Euclidean distance measure between an input vector x and c the center position of the radial unit or centroid.

The Moody and Darken transfer function, similar to a multivariate Gaussian density function, has been widely used as a radial basis function (Hassoun 1995). Thus, the output of a hidden node or the radial basis function node using the Moody-Darken transfer function is represented by (Haykin 1994):

$$g_k = \exp\left\{-\frac{\left\|x - c_k\right\|}{\sigma_k^2}\right\} \tag{14}$$

where:

g_k = output of the hidden node k and

σ_k = width of the radial unit.

In Eq. 13, *f(.)* is replaced by the Moody–Darken transfer function and can be written as (Bishop 1995):

$$y_i(x) = \sum_{k=1}^{M} w_{kj} g_k \tag{15}$$

where:

$j = 1, 2....Q$ (number of the output nodes) and

$k = 1, 2,...M$ (number of the nodes in the hidden layer).

Data pre-processing

Statistical and textural image features were extracted from 68 grid images. These features were used to train and test both NN models. A cross validation technique "leave-one-out" was applied to train and test the BPNN models following a similar approach described in Davis (1998), Spitz and Lek (1999), and Podnar et al. (2002). In this technique, there were a total of 67 observations in training and the remaining (one) observation was in testing. Hence, using successive training and testing cases, all observations were tested developing 67 independent training and testing data. The overall performance of the model was computed considering the average of all tested data. A similar approach was also performed for the RBFNN models.

Table 1. Performance of BPNN models with respect to RMSEP and minimum prediction accuracy for test data using leave-one-out approach.

Models	Input variables*	Root mean square error of prediction (%)	Minimum prediction accuracy (%)	Correlation coefficient (%)
BPGS	Green μ and σ	8.3	73.0	60
BPRS	Red μ and σ	8.0	72.0	57
BPNS	NIR μ and σ	10.0	64.0	58
BPGT	Green texture	8.3	75.5	59
BPRT	Red texture	8.3	74.5	62
BPNT	NIR texture	7.6	79.0	65
BPGvS	GVI μ and σ	8.6	76.5	54
BPNdS	NDVI μ and σ	8.0	71.0	63
BPGvT	GVI textures	8.3	70.5	66
PBNdT	NDVI texture	8.3	67.0	63

* μ and σ denote mean and standard deviation, respectively, for the respective band image features.

Table 2. Performance of RBFNN models with respect to RMSEP, prediction accuracies, and correlation coefficient for test data sets.

Models	Input variables*	Root mean square error of prediction (%)	Minimum prediction accuracy (%)	Correlation coefficient (%)
RBGS	Green μ and σ	8.6	75.3	56
RBRS	Red μ and σ	9.3	72.8	58
RBNS	NIR μ and σ	7.6	81.8	56
RBGT	Green texture	9.3	84.5	65
RBRT	Red texture	9.0	81.8	63
RBNT	NIR texture	8.3	81.9	67
RBGvS	GVI μ and σ	7.3	79.5	68
RBNdS	NDVI μ and σ	8.0	81.2	69
RBGvT	GVI textures	6.6	88.8	78
RBNdT	NDVI texture	7.0	83.7	70

* μ and σ denote mean and standard deviation, respectively, for the respective band image features.

Model development

The back propagation and radial basis function neural network models were developed and tested using neural network software (NeuralWare 2000). A total of ten BPNN models were developed. Table 1 shows these models and their associated input variables. The models that used textural information had five input nodes (each) representing five textural features associated with corresponding image bands. Similarly, the models that used global image statistical features had two inputs. Leaf nitrogen content expressed as percentage was the output of the NN models.

Table 2 shows ten RBFNN models developed for this study. Similar to the BPNN models, five models used textural features as inputs, each with five input nodes. The other five models used global image statistical features as inputs, each with two input nodes. The RBFNN models used the Moody-Darken transfer function. K-means clustering was used to determine the centroid and k-nearest neighbor heuristic was used to determine the width (σ_k) (Honavar and Uhr 1994; Hassoun 1995). A complete procedure for the image processing and neural network development is shown in Fig. 1.

Performance evaluation

Previous researchers have used an average accuracy or a root mean square error (RMSE) to measure the performance of neural network models (Sérélé et al. 2000; Thai and Shewfelt 1991). In our study, root mean square error of prediction, minimum prediction accuracy, and correlation coefficient were considered to evaluate the performance of neural network models. The root mean square error of prediction (RMSEP), minimum prediction accuracy (MPA), and correlation coefficient (r) were calculated from Eqs. 16-19.

$$P_i = \left[1 - \frac{\left|y_{ai} - y_{pi}\right|}{y_{ai}}\right] \times 100 \qquad (16)$$

$$RMSEP = \sqrt{\frac{\sum_{i=1}^{N}\left(y_{ai} - y_{pi}\right)^2}{N-1}} \qquad (17)$$

$$MPA = \min\left(P_1 \ldots\ldots\ldots P_N\right) \qquad (18)$$

$$r = \frac{\sum_{i=1}^{N}\left(y_{ai} - \bar{y}_a\right)\left(y_{pi} - \bar{y}_p\right)}{\sqrt{\sum_{i=1}^{N}\left(y_{ai} - \bar{y}_a\right)^2\left(y_{pi} - \bar{y}_p\right)^2}} \qquad (19)$$

where:

y_{ai}, y_{pi} = actual and predicted leaf nitrogen, respectively, and

$\bar{y}_a$, $\bar{y}_p$ = average of actual and predicted leaf nitrogen, respectively.

RESULTS and DISCUSSIONS

Tables 1 and 2 illustrate back propagation and radial basis function neural network models with their salient features and performance parameters. NN performance has been compared based on simultaneous comparison of three performance parameters i.e., root mean square error of prediction, minimum prediction accuracy, and correlation coefficient.

Performance of BPNN and RBFNN models based on statistical and textural image features

Of the six BPNN models (Table 1), the back propagation with textural features of NIR band (BPNT) model contributed the highest minimum prediction accuracy of 79% and the lowest root mean square error of prediction of 7.6%. The corresponding correlation between field observed and model predicted values was 65%, which was the second highest among

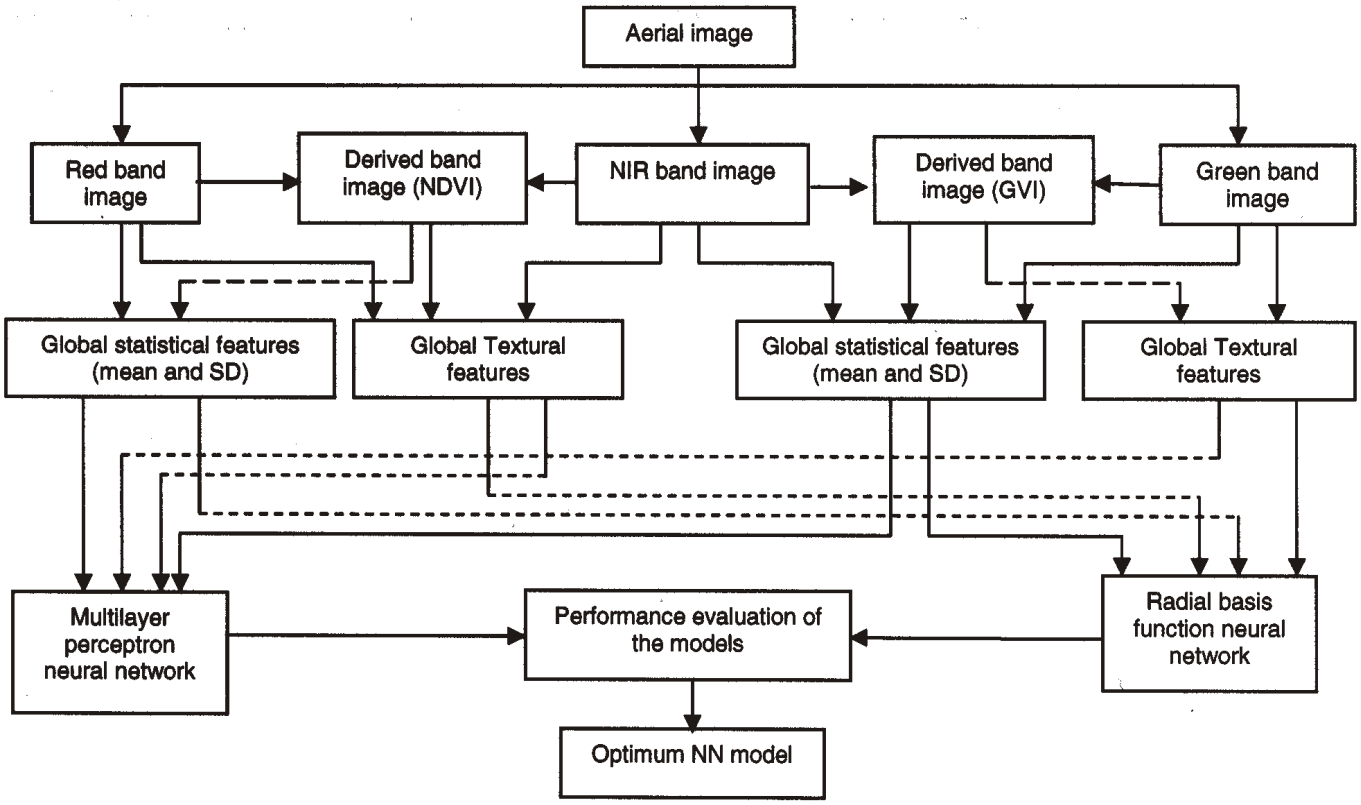

Fig. 1. Overall process involved to determine an optimal NN model from a set of potential neural network models for predicting leaf nitrogen content using aerial images under field conditions.

all statistical and textural features based on BPNN models. Similarly, of four BPNN models based on derived bands (BPGvS, BPNdS, BPGvT, and BPNdT), back propagation based on the green vegetation index global statistical features (BPGvS) model showed highest minimum prediction accuracy of 76.5%. On the other hand, the back propagation based on normalized difference vegetation index global statistical model (i.e., BPNdS) depicted the lowest root mean square error of 8%.

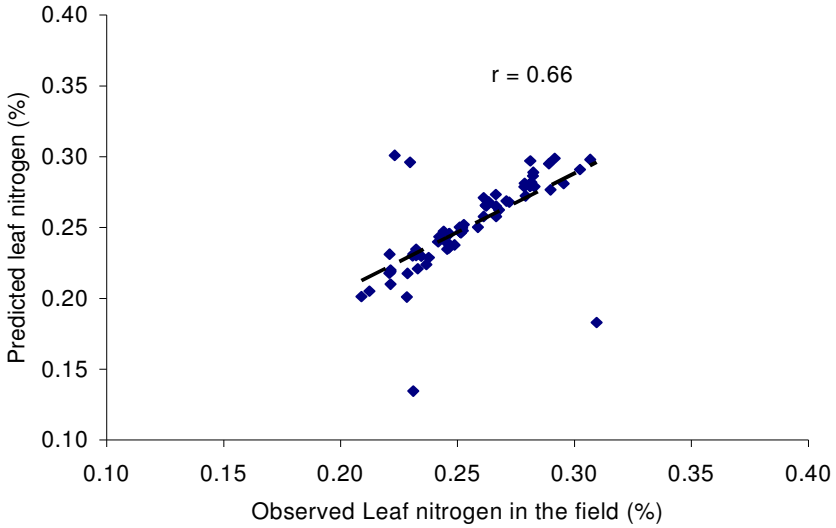

Fig. 2. Relationship between field observed leaf nitrogen and BPGvT model predicted leaf nitrogen.

Further, the highest correlation was from the BPGvT model (66%). Figure 2 illustrates the relationship between field observed leaf nitrogen and model predicted leaf nitrogen using the BPGvT model. It is clear that the model predicting leaf nitrogen resembles quite accurately the field observed leaf nitrogen.

Similarly, of the six RBFNN models (Table 2) based on individual band image information, the radial basis function based on green texture (RBGT) model yielded the highest minimum prediction accuracy of 84.5% and correlation coefficient of 65%. On the other hand, the model based on NIR texture, i.e., RBNT yielded slightly higher correlation (67%) than the RBGT model. In practice, both models seem to have equal performance in the real world conditions. The simultaneous comparison of three performance parameters clearly characterizes that the textural features of green as well as NIR band images consist of information on leaf nitrogen content under field conditions.

Again, of four RBFN models based on derived image features, the model based on green vegetation index i.e., RBGvT, had the lowest RMSEP (6.6%), highest minimum prediction accuracy (88.8%), and highest correlation coefficient (78%). It is also clear that the second highest performance is portrayed from the NDVI textural based

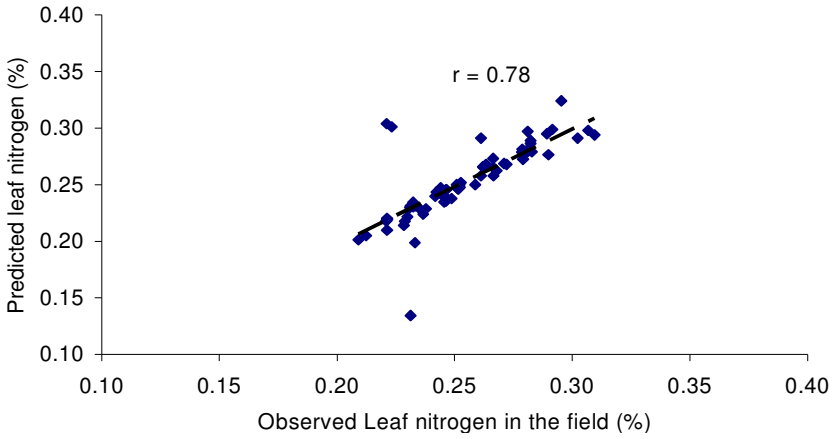

Fig. 3. Relationship between field observed leaf nitrogen and RBGvT model predicted leaf nitrogen.

model, i.e., RBNdT. Overall, the RBGvT model yielded the highest performance followed by the RBNdT model. Figure 3 delineates the correlation between the field observed and NN model predicted values. It is apparent that the model has the potential to predict spatial distribution patterns of leaf nitrogen under field conditions.

A comparison among the BPNN and RBFN based models showed that the majority of the RBFNN models manifested higher performance than those of the BPNN models. It is apparent that the models based on green and NIR textures yielded a higher performance than the models developed from other features, which is prevalent for both architectures. Moreover, the cross comparison also shows that the RBFN based models outperformed the BPNN based models. These findings indicated that the information from the green and NIR band statistical as well as textural features are highly correlated with leaf nitrogen content of corn plants under field conditions. Further, it was evident that the extracted textural image features provided more relevant information than the corresponding statistical features for predicting leaf nitrogen content under field conditions. These findings are similar to the previous study performed under corresponding field conditions (Beatty et al. 2000; Scharf and Lory 2000).

SUMMARY and CONCLUSIONS

An aerial image was acquired in multi-spectral bands (red, green, and NIR) for predicting leaf nitrogen content of corn under field conditions. Two additional image bands were derived using an appropriate transformation. The images were divided into 68 sub images as per the size of each field plot. Two statistical and five textural features were extracted from each sub-image. These image features were used as inputs to develop twenty neural network prediction models based on multilayer perceptron and radial basis function architectures. The model performance was evaluated using root mean square error of prediction, minimum prediction accuracy, and correlation coefficient.

When a neural network prediction model is used for real-world applications, it is difficult to comprehend a model with ideal performance (RMSEP of 0%, MPA of 100%, and r of 100%). The selection of the optimum model is ideally based on the simultaneous comparison of performance parameters that are used to delineate the model's accuracy. For this study, it is obvious that the best model would be the one that could provide the best performance from simultaneous comparison of the three performance parameters discussed above. Further, the implications of the comparison could go along with the significance and relevancy of the developed models. For this study, the model based on green vegetation index textural features i.e., RBGvT yielded the lowest RMSEP (6.6%), highest minimum prediction accuracy (88.8%), and highest correlation coefficient (78%). Hence, the resemblance of spectral information in green and NIR bands of the electromagnetic spectrum to corresponding leaf nitrogen content is inferred. Further validation of the models is recommended with respect to multiple years' datasets. Also, the models will need to be evaluated with respect to other research sites with diverse climatic conditions and crop varieties. Additional study could be conducted to rank NN models using appropriate statistical techniques.

ACKNOWLEDGEMENT

The authors acknowledge David Franzen, Associate Professor in the Soil Science Department, North Dakota State University for providing aerial images and the USDA-IFAFS program for financial support.

REFERENCES

Al-Abbas, A.H., R. Barr, J.D. Hall, F.L. Crane and M.F. Baumgardner. 1974. Spectra of normal and nutrient-deficient maize leaves. *Agronomy Journal* 66: 16-20.

Atkinson, P.M. and R.L. Tatnall. 1997. Neural networks in remote sensing: Introduction. *International Journal of Remote Sensing* 18 (4): 699-709.

Baldwin, A.H., K.L. McKee and I.A. Mendelssohn. 1996. The influence of vegetation, salinity, and inundation on seed banks of oligohaline coastal marshes. *American Journal of Botany* 83 (4): 470-479.

Beatty M.K., R. Caldanaro, C.J. Johanssen and K. Ross. 2000. In situ detection of leaf chlorophyll content and leaf nitrogen content in Zea Mays L. using remote sensing. *Proceedings of the Fifth International Conference on Precision Agriculture* (on CD). Madison, WI: American Society of Agronomy.

Behloul, F., B.P.F. Lelieveldt, A. Boudraa and J.H.C. Reiber. 2002. Optimal design of radial basis function neural networks for fuzzy-rule extraction in high dimensional data. *Pattern Recognition* 35: 659-675.

Benediktsson, J.A., P.H. Swain and O.K. Ersoy. 1990. Neural network approaches versus statistical methods in classification of multisource remote sensing data. *IEEE Transactions on Geoscience and Remote Sensing* 28: 540-552.

Bettinger, P., G.A. Bradshaw and G.W. Weaver. 1996. Effects of geographic information system vector-raster-vector data conversion on landscape indices. *Canadian Journal of Forest Research* 26 (8): 1416-1425.

Bishop, C.M. 1995. *Neural Networks for Pattern Recognition.* Oxford, England: Clarendon Press.

Black, C.A. 1999. *Soil Fertility Evaluation and Control.* Boca Raton, FL: Lewis Publishers.

Blackmer A. and S.E. White. 1998. Using precision farming technologies to improve management of soil and fertilizer nitrogen. *Australian Journal of Agricultural Resource* 49: 555-564.

Blackmer, T.M., J.S. Shepers, G.S. Varvel and E. Water-Shea.1996. Nitrogen deficiency detection using reflected short wave radiation from irrigated corn canopies. *Agronomy Journal* 88: 1-5.

Bogdanov, A.V., S. Sandven, O.M. Johannessen, V.Y. Alexandrov and L.P. Bobylev. 2005. Multisensor approach to automated classification of sea ice image data. *IEEE Transactions on Geoscience and Remote Sensing* 43 (7): 1648-1664.

Brown, M. and C.J. Harris. 1994. *Neurofuzzy Adaptive Modeling and Control*. New York, NY: Prentice Hall.

Chen, S., C.F.N. Cowan and P.M. Grant. 1991. Orthogonal least squares learning algorithm for radial basis function networks. *IEEE Transactions on Neural Networks* 2(2): 302-309.

Cichocki, A. and R. Unbehauen. 1993. *Neural Networks for Optimization and Signal Processing*. Chichester, NY: John Wiley & Sons.

Cihacek, L.J. and T.A. Kerby. 1991. Effects of residual soil nitrogen and urea on yield and petiole nitrate of cotton. *Journal of Production Agriculture* 4:193-197.

Critten, D.L. 1997. Fractal dimension relationships and values associated with certain plant canopies. *Journal of Agricultural Engineering Research* 67 (1): 61-72.

Davis, A.M.C. 1998. Cross validation: Do we love it too much? *Spectroscopy Europe* 10 (2): 24-25.

Diker, K., D.F. Heermann, W.C. Bausch and D.K. Wright. 2004. Shannon-Wiener's diversity index for linking yield monitor and remotely sensed data for corn. *Transactions of the ASAE* 47(4): 1347-1354.

Drummond, S.T., K.A. Sudduth, A. Joshi, S.J. Birrell and N.R. Kitchen. 2002. Statistical and neural methods for site-specific yield prediction. *Transactions of the ASAE* 47 (1): 5-14.

Fernandez, A., P. Illera and J.L. Casanova. 1997. Automatic mapping of surfaces affected by forest fires in Spain using AVHRR NDVI composite image data. *Remote Sensing Environment* 60 (2): 153-162.

Filella, I., L. Serrano, J. Serra and J. Penuelas. 1994. Crop ecology production and management: Evaluating wheat nitrogen status with canopy reflectance indices and discriminant analysis. *Crop Science* 35: 1400-1405.

Flowers, M., R. Weisz and R. Heiniger. 2000. Aerial photographic determination of nitrogen application timing and rate recommendations in winter wheat. *Proceedings of the Fifth International Conference on Precision Agriculture* (on CD). Madison, WI: American Society of Agronomy.

Foody, G.M. 1995a. Using prior knowledge in artificial neural network classification with a minimal training set. *International Journal of Remote Sensing* 16: 301-312.

Foody, G.M. 1995b. Land cover classification using an artificial neural network with ancillary information. *International Journal of Geographical Information Systems* 9: 527-542.

Gaston, G.G., P.M. Bradley, T.S. Vinson and T.P. Kolchugina. 1997. Forest ecosystem modeling in the Russian Far East using vegetation and land-cover regions identified by classification of GVI. *Photogrammetry Engineering and Remote Sensing* 63 (1): 51-58.

Goodin, D.G. and G.M. Henebry. 1997. A technique for monitoring ecological disturbance in tallgrass prairie using seasonal NDVI trajectories and a discriminant function mixture model. *Remote Sensing Environment* 61 (2): 270-278.

Greenwood, D.J., F. Gastal, G. Lemaire, A. Draycott, P. Millard and J.J. Neeteson. 1991. Growth rate and % N of field grown crops: Theory and experiments. *Annals of Botany* 67: 181-190.

Haralick, R.M., K. Shanmugam and I. Dinstein. 1973. Textural features for image classification. *IEEE Transactions on Systems, Man, and Cybernatics* 3 (6): 610-621.

Hassoun, M.H. 1995. *Fundamentals of Artificial Neural Networks*. Cambridge, MA: MIT Press.

Haykin, S. 1994. *Neural Networks*, 1st edition. New Jersey, NJ: Prentice Hall Inc.

Honavar, V. and L. Uhr. 1994. *Artificial Intelligence and Neural Networks*: *Steps towards Principled Integration.* Boston, MA: Academic Press.

Hong, N.J., S. Rim, J. Lee and J. Kim. 1997. Remote sensing for estimating chlorophyll amount in rice canopies. *Proceedings of 1997 IEEE International Geoscience and Remote Sensing Symposium* 1: 89-91.

Huang, D. S. 1999. Radial basis probabilistic neural networks: Model and application. *International Journal of Pattern Recognition and Artificial Intelligence* 13(7): 1083-1101.

Huemmrich, K.R. and S.N. Goward. 1997. Vegetation canopy PAR absorptance and NDVI: An assessment for ten tree species with the SAIL model. *Remote Sensing Environment* 61(2): 254-269.

Huggins, D.R. and W.L. Pan. 1993. Nitrogen efficiency component analysis: An evaluation of cropping system differences in productivity. *Agronomy Journal* 85: 898-905.

Idrisi32.11. 2000. *Guide to GIS and Image Processing*, volumes 1-2. Worcester, MA: Clark Labs.

Lecain, D.R., J.A. Morgan, G.E. Schuman, J.D. Reeder and R.H. Hart. 2002. Carbon exchange and species composition of grazed pastures and exclosures in the shortgrass steppe of Colorado. *Agricultural Ecosystem and Environment* 93 (1/3): 421-435.

Majumdar, S. and D.S. Jayas. 1999. Classification of bulk samples of cereal grains using machine vision. *Journal of Agricultural Engineering Research* 73: 35-47.

Monmonier, M.S. 1974. Measures of pattern complexity for cholopleth maps. *The American Cartographer* 1: 159-169.

NeuralWare. 2000. Professional II/Plus tool kit, *Reference Manual*. Carnegie, PA: NeuralWare.

O'Neal, M.R., B.A. Engel, D.R. Ess and J.R. Frankenberger. 2002. Neural network prediction of maize yield using alternative data coding algorithm. *Biosystems Engineering* 83(1): 31-45.

Pachepsky, V., A.D. Timlin and G.Varallyay. 1996. Artificial neural networks to estimate soil water retention from easily measurable data. *Soil Science Society of America Journal* 60(3): 727-733.

Pal, N.R., S. Pal, J. Das and K. Majumdar. 2003. SOFM-MLP: A hybrid neural network for atmospheric temperature prediction. *IEEE Transactions on Geoscience and Remote Sensing* 41(12): 2783-2791.

Plate, T., J. Bert, J. Grace and P. Band. 2000. Visualizing the function computed by a feed forward neural network. *Neural Computation* 12(6): 1355-1370.

Podnar, D., D. Koracin and A. Panorska. 2002. Application of artificial neural networks to modeling the transport and dispersion of tracers in complex terrain. *Atmospheric Environment* 36: 561-570.

Reeves, D.W., P.L. Mask, C.W. Wood and D.P. Delaney. 1993. Determination of wheat nitrogen status with a hand held chlorophyll meter: Influence of management practices. *Journal of Plant Nutrition* 16(5): 781-796.

Sauchelli, V. 1964. *Fertilizer Nitrogen: Its Chemistry and Technology*. New York, NY: Reinhold Publishing Corp.

Schalkoff, R. 1992. *Pattern Recognition: Statistical, Structural, and Neural Approaches*. New York, NY: Wiley Publishing.

Scharf, P.C. and J.A. Lory. 2000. Calibration of remotely sensed corn color to predict nitrogen need. *Proceedings of the Fifth International Conference on Precision Agriculture* (on CD). Madison, WI: American Society of Agronomy.

Sérélé, C.Z., Q.H.J. Gwyn, J. Boisvert, E. Pattey, N. McLaughlin and G. Daoust. 2000. Corn yield prediction with artificial neural network trained using airborne remote sensing and topographic data. *Proceedings of 2000 IEEE International Geoscience and Remote Sensing Symposium* 1: 384-386.

Shackleton, C. 2002. Nearest-neighour analysis and the prevelance of woody plant competition in South African savannas. *Plant Ecology* 158 (1): 65-76.

Sheftel, B.I. and I. Hanski. 2002. Species richness, relative abundances and habitat use in local assemblages of Sorex shrews in Eurasian boreal forests. *Acta Theriologica* 47 (1): 69-79.

Spitz, F. and S. Lek. 1999. Environmental impact prediction using neural network modeling: An example in wildlife damage. *Journal of Applied Ecology* 36: 317-326.

Stone, M.L., J.B. Solie, W.R. Raun, R.W. Winey, S.L. Taylor and J.D. Ringer. 1996. Use of spectral radiance for correcting in-season fertilizer nitrogen deficiencies in winter wheat. *Transaction of the ASAE* 39 (5): 1623-1631.

Thai, C.N. and R.L. Shewfelt. 1991. Modeling sensory color quality of tomato and peach: Neural networks and statistical regression. *Transactions of the ASAE* 34(3): 950-955.

Tumbo, S.D., D.G. Wagner and P.H. Heinemann. 2002. Hyperspectral-based neural network for predicting chlorophyll status in corn. *Transactions of the ASAE* 45 (3): 825-832.

Turner, M.G. 1989. Landscape ecology: The effect of pattern on process. *Annual Revision of Ecological Systems* 20: 171-197.

Viets, F.G. and R.H. Hageman. 1971. Factors affecting the accumulation of nitrate in soil, water, and plants. *Agriculture Handbook No. 413*. Washington, DC: Agricultural Research Service, USDA.

Yang, C.C., S.O. Prasher and R. Lacroix. 1996. Applications of artificial neural networks to land drainage engineering. *Transactions of the ASAE* 39(2): 525-533.

Zhuang, X. and A.E. Bemard. 1990. Classification of multispectral remote sensing data using neural network vs statistical methods. *ASAE Paper No. 90-7552*. St Joseph, MI: ASABE.